Journal of Science and Technology in Civil Engineering, HUCE (NUCE), 2022, 16 (1): 1–18

EFFECT OF PRESTRESSING FORCE ON FLEXURAL BEHAVIOR OF UNBONDED PRESTRESSED CONCRETE BEAMS STRENGTHENED BY CFRP SHEETS

Dang Dang Tung[a,b], Chu Van Tu[a,b], Huynh Thi Kim Phung[a,b], Nguyen Minh Long[a,b,*]

[a] *Faculty of Civil Engineering, Ho Chi Minh City University of Technology (HCMUT), 268 Ly Thuong Kiet street, District 10, Ho Chi Minh city, Vietnam*
[b] *Vietnam National University Ho Chi Minh City (VNU-HCM), Linh Trung Ward, Thu Duc city, Ho Chi Minh city, Vietnam*

Article history:
Received 07/12/2021, Revised 13/01/2022, Accepted 14/01/2022

Abstract

This paper presents an experimental study on the effect of prestressing force on the flexural behavior of unbonded prestressed concrete (UPC) strengthened by Carbon fiber reinforced polymer (CFRP) sheets. The testing program was carried out on nine large-scale UPC rectangular beams. The investigated parameters included the reduction of prestressing force (0%, 15%, and 30%) and the number of CFRP layers (0, 2, and 4 layers). Experimental results showed that the strengthening effectiveness of CFRP sheets, controlling cracking, and the energy absorption capacity tended to increase with the decrease of prestressing force and decrease with the increase of the CFRP sheets ratio. The effective performance of the CFRP sheets was shown by the increase in the strain of the CFRP sheets which was proportional to the decrease in the prestressing force. The CFRP sheets strongly interacted with tendons, significantly decreased the tendon strain, and delayed the point where nominal yield strain in tendons occurred; this reduction was significant when the prestressing force was small. Besides, the reduction in prestressing force considerably increased the displacement of beams and the additional strain of the tendons (up to 164%), but this increase became smaller as the number of CFRP layers increased.

Keywords: flexural strength; unbonded prestressed concrete (UPC) beams; prestressing force; CFRP sheets; strengthening effectiveness; interaction between CFRP sheets and tendons; number of strengthening layers.

https://doi.org/10.31814/stce.huce(nuce)2022-16(1)-01

1. Introduction

Unbonded prestressed concrete (UPC) members with advantages such as economical (due to not having to spend time and expenses on tendon grouting), low prestress losses due to low friction, changeable and monitorable during service, that have proved to be an effective structural solution besides bonded prestressed concrete (BPC) members and have been applying since the 1960s in USA, Australia, Europe, and Asia [1, 2]. After a long period of usage, in order to prolong the service life, UPC members need to be strengthened due to the material degradation, prestress losses or the requirement of technical quality improvement. To meet this demand, several traditional strengthening methods commonly currently used for BPC or UPC structures can be mentioned as increasing cross-section area by adding an extra layer of reinforced concrete (RC), installing steel plate on the tension

*Corresponding author. *E-mail address:* nguyenminhlong@hcmut.edu.vn (Long, N. M.)

face, and installing external tendons. The first method, increasing cross-section area with RC, may be inapplicable in cases that require preserving the architectural functions, and the aesthetics of the construction. External tendons require difficult techniques and may not be applicable in old, weak, or heavily damaged structures; while externally bonded steel plate technique may have difficulties in structures that dwell in highly corrosive areas (due to steel's susceptibility to corrosion), or in structures with restricted space that makes the arranging lifting steel equipment which is also heavy to be difficult. All these factors contribute to the rising cost of construction [3]. Due to the superior technical characteristics of CFRP materials such as high strength, light specific gravity, non-conductive, non-magnetic, non-corrosive, simple construction method, the solution of using CFRP materials for retrofit or strengthening of BPC and UPC structures has shown its high efficiency besides existing traditional solutions [4–8].

While researches on flexural strengthening of BPC members with externally bonded CFRP under monotonic [9–18] or repeated load [19–23] began approximately 17 years ago, researches related to analyzing the effectiveness of flexural strengthening of UPC members began much later and are still very few in numbers. [6, 24–29]. In BPC beams flexural strengthened with CFRP sheets, tendons and surrounding concrete maintain the integrity, thus the strain compatibility condition in tendons, concrete, and CFRP sheets is satisfied, which leads to a relatively uniform interaction between the tendons and the surrounding concrete along the beam. Meanwhile, the strain of tendons in UPC beams is not compatible with the strain of concrete and CFRP sheets, as the tendons do not work simultaneously with concrete and CFRP sheets. In this case, the interaction of unbonded tendons, the surrounding concrete, and FRP sheets does not uniformly occur along the beam; rather, they only work together locally, through the prestressing force at the two anchorage ends. This may lead to a significant diffrence in the flexural strengthening efficiency of UPC beams as compared to that of UPC beams [6, 28, 29]. The lack of researches on BPC beams strengthened with CFRP sheets could be the reason there is a lack of design provisions for UPC structures in current design guidelines for strengthening using FRP materials, such as ACI 440.2R [30], CNR DT200R1 [31], and TR 55 [32].

Regarding PC members in general and UPC members in particular, the long periods of use usually leads to a reduction of prestressing force in tendons due to an increase in prestress losses such as relaxation of tendons, anchorage slip, or tendon corrosion. In BPC members, the changes in tendon's prestressing force significantly impact the ability of crack control, flexural capacity, stiffness, crack behavior and the ductility of beams [33, 34], as well as long-term prestress losses due to creep and shrinkage [35]. In UPC members, changes in prestressing force also impact cracking patterns (number of cracks, the width of cracks, and spacing between cracks) and failure mode [36, 37]. The aforementioned changes in cracking patterns or cracking behavior and failure modes of UPC beams due to changes in prestressing force could significantly impact the strain and the debonding of CFRP sheets when CFRP sheets are tightly bonded to the tension face of the member, thus affecting the perfomence and strengthening effectiveness of CFRP sheets. In previous studies concerning flexural behavior of UPC members strengthened with CFRP sheets have mentioned above, [25] is the only paper that investigates the tendon ratio (prestressing force); however, this paper does not mention and explicitly conclude the effects of prestressing force on strengthening effectiveness of CFRP sheets, and the interaction between prestressing force and strain of CFRP sheets. It is important to clarify these interactions, which can help to build safe and reasonable calculation provisions for designing UPC members strengthened with externally bonded CFRP sheets in the contexts that there is a lack of design provisions for UPC members using CFRP sheets in current standards as mentioned above.

This paper presents an experimental study on the effect of prestressing force on the flexural behavior of UPC beams strengthened by CFRP sheets. The testing program was carried out on nine large-scale UPC rectangular beams. The investigated parameters included the reduction of prestressing force (0%, 15%, and 30%) and the number of CFRP layers (0, 2, and 4 layers). The main objective of this paper is to clarify the effects of prestressing force on the flexural behavior of UPC beams strengthened by CFRP sheets, and to evaluate the effects of prestressing force on the interaction between tendons and CFRP sheets.

2. Experimental investigation

2.1. Materials and preliminary tests

The mixture design of concrete are presented in Table 1, included: PC40 cement (435 kg/m^3); coarse aggregates (22 mm, 931 kg/m^3); coarse sands (0 ÷ 4 mm, 516 kg/m^3); fine sands (0 ÷ 2 mm, 351 kg/m^3); and superplasticize (5.4 l/m^3). The average axial compressive strength $f_{c,cube}$ and tensile strength $f_{sp,cube}$ of the concrete was determined on 6 concrete cubes 150×150×150 mm, with $f_{c,cube}$ = 47.2 MPa and $f_{sp,cube}$ = 5.8 MPa. The concrete slump was approximately 12±2 cm. The yield strength f_y and ultimate tensile strength f_u of the longitudinal rebars and steel stirrups were determined on three samples, with the following result: f_y = 430 MPa and f_u = 600 MPa; the stirrups had f_{yw} = 342 MPa and f_{uw} = 463 MPa. The rebar had Elastic modulus of E_s = 200 GPa. The unbonded tendons were 7-wire strands with nominal diameter of 12.7 mm, and nominal yield strength f_{py} and the nominal ultimate strength f_{pu} were 1675 MPa and 1860 MPa respectively. The Elastic modulus of the tendons was E_p = 195 GPa. The unidirectional CFRP sheet (CFF) had the nominal thickness of 0.166 mm, the ultimate tensile strength f_{fu} = 4900 MPa, the elastic modulus E_f = 240 GPa, and the rupture strain ε_{fu} = 2.1%. The epoxy resin (included two parts, A and B) had the tensile strength $f_{epoxy,u}$ = 60 MPa, the elastic modulus E_{epoxy} in the range of 3 to 3.5 GPa. The mechanical properties of concrete, tendons, CFRP sheets, and rebar are presented in Table 2.

Table 1. Concrete mix design

Constituent	Unit	Quantity
PC40 cement	kg/m^3	435
Coarse aggregates (22 mm)	kg/m^3	931
Coarse sands (0 ÷ 4 mm)	kg/m^3	516
Fine sands (0 ÷ 2 mm)	kg/m^3	351
Superplasticize	l/m^3	5.4

Table 2. Mechanical properties of concrete, tendon, CFRP sheets and rebar

Concrete		Tendon^a		CFRP^a				Longitudinal rebars			Steel stirrups	
$f_{c,cube}$ (MPa)	$f_{sp,cube}$ (MPa)	f_{pu} (MPa)	f_{py} (GPa)	E_p (%)	f_{ffu} (MPa)	E_f (GPa)	ε_{ffu} (%)	f_u (MPa)	f_y (MPa)	E_s (GPa)	f_{uw} (MPa)	f_{yw} (MPa)
47.2	5.8	1860	1675	195	4900	240	2.1	600	430	200	463	342

Note: ^{a}Value provided by manufacturers.

2.2. Beam design

The experimental program was conducted on nine large-scale UPC rectangular beams, 120 × 360 × 4000 mm, with the scale of 1 : 3 compared to the actual beam (beam span). The beams were divided into three groups: Group 1, Group 2, and Group 3 (Table 3). These beams were designed to analyze the effect of the decrease of prestressing force on flexural behavior of UPC beams strengthened with CFRP sheets, corresponding to three reduction levels of prestressing force: 0%, 15%, and 30%, not accounting for tendon corrosion based on Naaman (2004) proposal [38], and accounting for tendon corrosion based on O'Flaherty et al. (2017) proposal [39]. Each group consists of three beams, in which one un-strengthened beam (as a reference beam) and the two were strengthened with longitudinal CFRP sheets installed along the bottom of the beam, with numbers of CFRP layers of 2 and 4 layers, respectively; these were anchored with CFRP U-wrapped uniformly distributed within the shear span to restrict the early debonding of longitudinal CFRP sheets. After 28 days from casting, the beams were post-tensioned by one unbonded 7-wire strands with the nominal diameter of 12.7 mm, following a curved trajectory (Fig. 1). The initial prestressing forces of the three groups 1, 2, and 3 were 128.5 kN, 109.2 kN, and 90 kN respectively (corresponding to the initial stresses of 1302 MPa, 1107 MPa and 911.4 MPa respectively in tendons). The beams were designed according to ACI 318 [40] class U with uncracked section. Thus, the initial prestressing forces were calculated so that the following condition is satisfied $f_t < 0.62\,(f_c')^{0.5}$, in which f_t is the maximum tensile stress in concrete, and f_c' as the compressive strength of concrete determined from cylinders. The tension side and compression side of the beam were arranged with two 12 mm bars and two 10 mm bars respectively. Stirrups had the diameter of 6 mm, the distance between stirrups in shear span and load span were 125 mm and 150 mm, respectively. At the two ends, within 300 mm, in order to avoid possible local damages due to prestressing force, the stirrups were distributed more densely with a distance of 50 mm. The dimensions, tendon specifications, rebar specifications, and CFRP sheets specifications are given in Table 2 and Table 3. The cross section, distribution of tendons, rebars, and CFRP strengthening schemes are given in Fig. 1 and Fig. 2.

Table 3. Summary of test parameters

No.	Group	Specimen	Dimensions (mm)	$f_{c,cube}$ (MPa)	L_s (%)	n_{FRP}	t_f (mm)	w_f (mm)
1	1	P.B0-Cont	120×360×4000	47.2	0	0	-	-
2		P.B0-2CB			0	2	0.166	100
3		P.B0-4CB			0	4	0.166	100
4	2	P.B1-Cont			15	0	-	-
5		P.B1-2CB			15	2	0.166	100
6		P.B1-4CB			15	4	0.166	100
7	3	P.B2-Cont			30	0	-	-
8		P.B2-2CB			30	2	0.166	100
9		P.B2-4CB			30	4	0.166	100

Note: L_s is the reduction level of prestressing force, %; $f_{c,cube}$ is the compressive strength of concrete cubes, MPa; n_{FRP} is the number of CFRP layers; t_f is the thickness of one ply of CFRP sheet, mm; w_f is the width of flexural-strengthening CFRP sheets, mm.

The installation of CFRP sheets were conducted one day after tensioning the beams. Before bonding with CFRP sheets, the concrete surface where to be strengthened was ground with a handheld grinding machine, until touching the aggregates. The voids on the to-be-strengthened surface were filled with epoxy resin and then smoothed out again. Dust accumulated on the concrete surface were vacuumed. Epoxy was mixed according to manufacturer's instruction and was applied to the to-be-strengthened surface using a roller; after that, CFRP sheet was applied on the surface of epoxy layer. Another layer of epoxy layer was then spread on top of the CFRP sheet using a roller with enough pressure to ensure good bonding between the CFRP sheet and the concrete surface. The roller was used regularly to even out the strengthening sheets' surface and to eliminate air bubbles in the epoxy layer, until the strengthening sheet was saturated. The whole process took place in a laboratory with an average temperature of 29 °C, and humidity of approximately 75%. The time it took for CFRP sheets to reach maximum strength was 7 days.

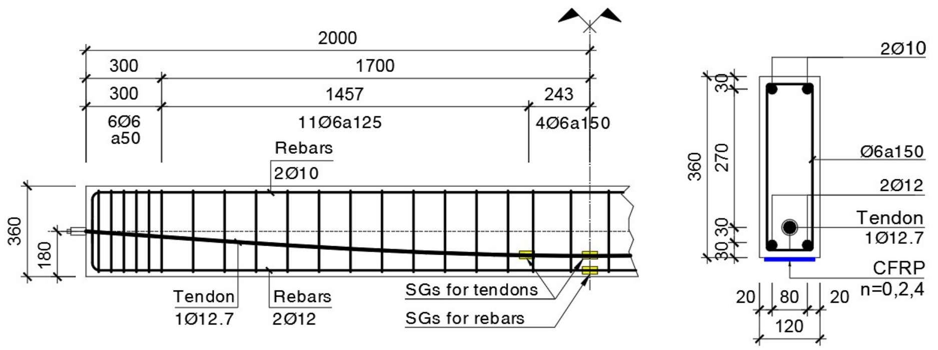

Figure 1. Details of the tested beams: (a) Arrangement of tendons, rebars, stirrups and strain gauges (SGs); (b) Beam section at midspan

2.3. Test procedure and instrumentation

All beams were tested using 4-point bending test as shown in Fig. 2 and Fig. 3. The position of the applied load was 1457 mm away from the nearest support. The strain of longitudinal CFRP sheets along the beam span was measured by using four strain gauges (SGs) attached to the surface of the sheets at the midspan (two SGs) and at the two loading points. The strain of unbonded tendon was monitored through three SGs in the constant moment zone. The strain of longitudinal bar in tension face was determined through one SGs attached at the midspan. The strain of concrete was measured using five SGs attached to the beam's compression side and tension side at the midspan along the height of the section. The beam displacement was determined through five linear variable differential transformers (LVDTs) placed at the midspan, the loading points, and the supports. The beams were tested under load step of 5 − 10 kN before flexural cracks appear, after that, each load step would increase by 15 − 20 kN. After reaching each load step, the load was maintained in around three minutes to measure displacement, strain of

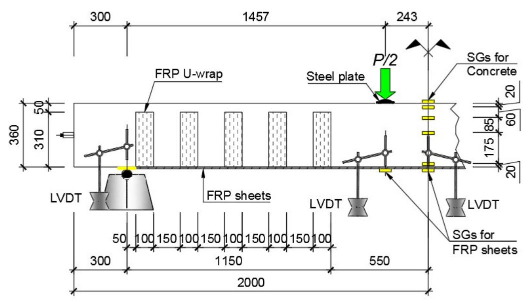

Figure 2. Test setup and instrumentation details

concrete, longitudinal rebar, CFRP sheets, and width of cracks. All the load values, displacement, and strain are automatically measured through the receiving devices. The layout and location of instrumentation are shown in Fig. 1 and Fig. 2.

Figure 3. Tested beam in the laboratory

3. Test result and discussion

3.1. Cracking pattern and failure mode of tested beams

The test results of all beams are summarized in Table 4. The un-strengthened beam in the group with no prestressing force reduction (Group 1) failed because flexural failure with the tendon strain exceeded the nominal yield strength, and after that concrete in the compressive zone was ruptured at the midspan (Fig. 4(a)). The un-strengthened beams in the group with prestressing force reduction of 15% (Group 2), and 30% (Group 3) also failed because flexural failure with concrete in the compressive zone was ruptured at the midspan. The failure mode of the un-strengthened beams was more brittle than that of the strengthened beams, as shown through the quicker development of cracks, with fewer but wider cracks. The first flexural crack appeared at the midspan at the load level of approximately 47 – 50% of its maximum load. The width of cracks at the maximum load was approximately 3.0 – 3.8 mm.

Table 4. Test results

Group	Beam	L_s (%)	$P_{cr,exp}$ (kN)	$P_{u,exp}$ (kN)	$\delta_{u,mid}$ (mm)	ε_{cu} (‰)	ε_{pu} (‰)	ε_{su} (‰)	ε_{fu} (‰)	E_b (Nmm $\times 10^3$)	Failure mode
1	P.B0-Cont	0	45	89.7	33.7	3.0	9.1	34.5		2406	TY-C
	P.B0-2CB		50	142.7	38.7	3.4	9.5	26.7	11.8	3946	TY-C-BR
	P.B0-4CB		50	165.7	38.0	3.1	9.0	23.5	9.1	4252	TY-C-BR
2	P.B1-Cont	15	40	85.1	38.4	3.1	8.5	40.1		2648	C
	P.B1-2CB		45	137.5	40.8	4.0	8.4	33.5	11.6	4025	C-R
	P.B1-4CB		45	153.8	39.4	2.8	8.5	21.5	9.8	4198	C-BR
3	P.B2-Cont	30	36	77.3	30.1	3.3	8.4	20.5		1697	C
	P.B2-2CB		40	133.3	44.1	3.1	9.4	22.3	13.2	4200	TY-C-R
	P.B2-4CB		40	147.4	34.3	2.5	7.6	15.1	9.2	3352	C-BR

In which: TY – tendon yielding; C – concrete crushing at compression side; R – rupture of CFRP sheets; BR – debonding and spliting of CFRP sheets.

Note: L_s is the prestressing force reduction level, %; $P_{cr,exp}$ and $P_{u,exp}$ are cracking load and maximum load at failure respectively, kN; $\delta_{u,mid}$ is beam deflection at midspan at failure, mm; ε_{cu} and ε_{su} are the maximum compressive concrete strain and the maximum tensile strain in rebars at midspan respectively, ‰; ε_{pu} and ε_{fu} are maximum tensile strain in tendons and of CFRP sheets at midspan respectively, ‰; E_b is energy absorption capacity, Nmm $\left(\times 10^3\right)$.

Energy absorption capacity, E_b, is defined as the area below the load-displacement curves up to the maximum loads. The above results showed that CFRP helped to improve the ductility of beams, which is an important structural characteristic, especially in the case of the beams subjected to dynamic loads; especially, this increase is directly proportional to the decrease in prestressing force.

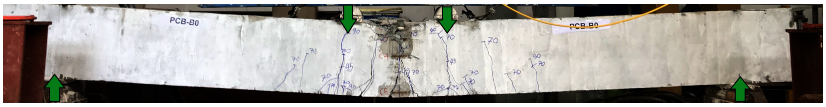

(a) P.B0-Cont

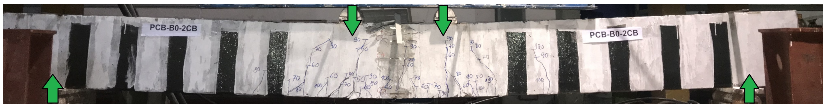

(b) P.B0-2CB

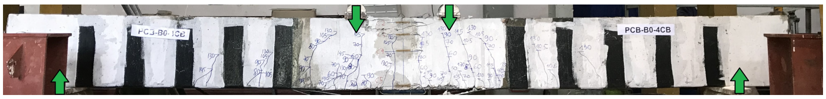

(c) P.B0-4CB

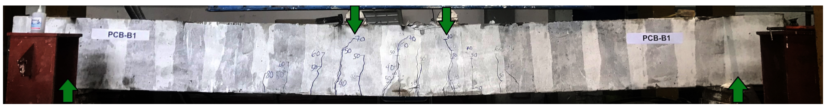

(d) P.B1-Cont

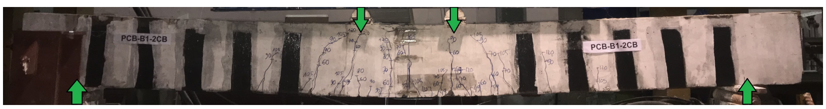

(e) P.B1-2CB

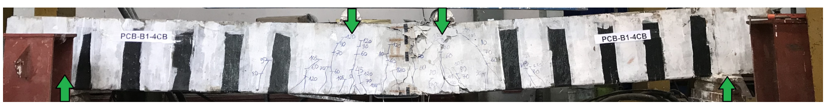

(f) P.B1-4CB

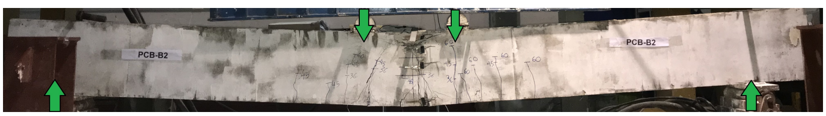

(g) P.B2-Cont

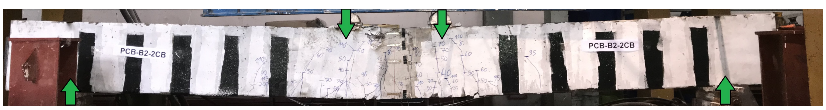

(h) P.B2-2CB

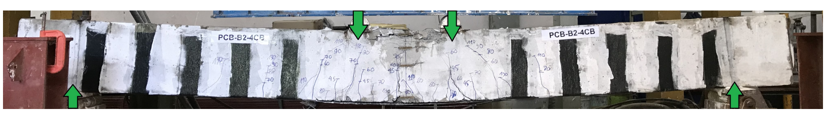

(i) P.B2-4CB

Figure 4. Cracking pattern and failure mode of the tested beams

3.2. Load-deflection relationships

The load-deflection relationship of the tested beams is shown in Fig. 5. This relationship could be divided into two periods. In the period from the first load to the cracking loads of the un-strengthened beams (P-Cont beams), $P_{cr} = (0.5, 0.45, 0.4)\,P_{u,0}$ (corresponding to the un-strengthened beams in Group 1, 2, 3 respectively) where $P_{u,0}$ is the maximum load of the un-strengthened beams in Group 1 (beam P.B0-Cont), the beams behaved linearly and there was almost no difference (Fig. 5). In this period, the prestressing force reduction and CFRP sheets had almost no impact on the beam behavior. In the later period, from the load levels $P_{cr,0}$ to the failure load, the appearance and development of cracks led to a decrease in the stiffness of the beams and the beam deflection also increased with a higher rate. The increase rates of deflection was directly proportional with prestressing force reduction; however, inversely proportional with the number of CFRP sheets. In this period, the flexural-strengthening CFRP sheets showed their ability to control and delay crack development, postponing the degradation of the stiffness of the strengthened beams, thereby reducing the beam deflection of the strengthened beams compared to that of the reference beam at the same load level.

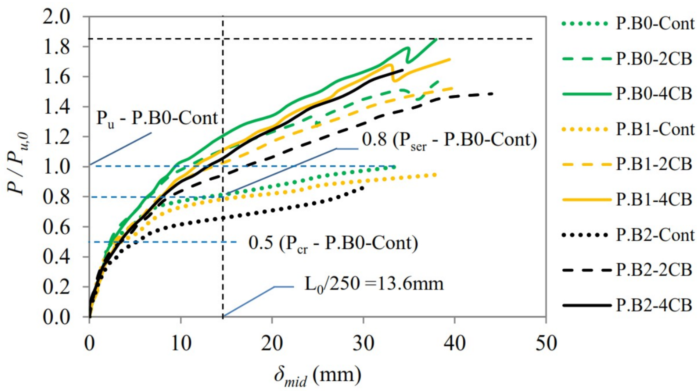

Figure 5. Relative load-deflection relationships at mid-span of the tested beams

At the allowable load at the serviceability state of un-strengthened beams (load level that caused the displacement $= L/250 = 13.6\,\text{mm}$), $P_{ser} = (0.8, 0.77, 0.65)\,P_{u,0}$ (corresponding to the un-strengthened beams in Group 1, 2, and 3), the displacement of the beams strengthened with 2 and 4 CFRP layer decreased by 50% to 51% in Group 1 (no prestressing force reduction), 44 – 46% in Group 2 (15% prestressing force reduction) and 56 – 59% in Group 3 (30% prestressing force reduction). Likewise, at maximum load of the un-strengthened beams, $P_{u,cont}$, the displacement of the beams strengthened with 2 and 4 CFRP layers decreased 68% and 72% in Group 1 (no prestressing force reduction); 70% and 73% in Group 2 (15% prestressing force reduction); and 63% and 69% in Group 3 (30% prestressing force reduction). This result showed that beam displacement reduction only improved a little when the number of CFRP layers increased from 2 to 4 layers.

The effect of prestressing force reduction levels on beam displacement is shown in Fig. 6. Considering the strengthened beams with the same number of CFRP layers, in the first period before beam displacement exceeded allowable displacement ($L/250 = 13.6\,\text{mm}$), beams with different prestressing force reduction exhibited almost the same behavior. In the next load levels when beam displacement exceeded allowable limits, beam displacement increased in accordance with prestressing force reduction levels. In particular, at the maximum loads of beams with prestressing force reduction (beams in Group 2 and 3), displacement of these beams increased when compared to the beams with no prestressing force reduction (Group 1), the value were 43% and 56% for the un-strengthened beams, 9% and 35% for the beams strengthened with 2 CFRP layers, 6% and 13% for the beams strengthened with 4 CFRP layers. An increase in beam displacement could be due to prestressing force reduction which led to a decrease in beam stiffness. Besides, when the number of layers increased, the increase level in beam displacement (due to prestressing force reduction) tended to decrease. This could be due to the excellent cracking control mechanism of CFRP sheets that helped to constraint the rate of increase in deflection.

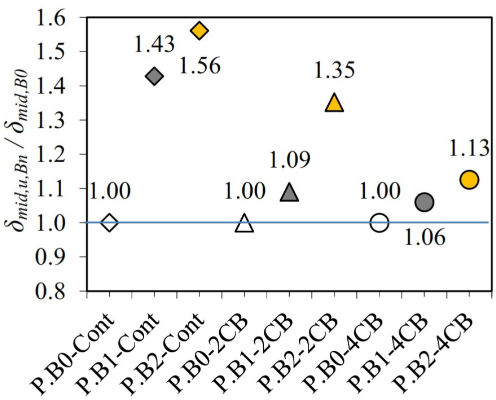

Figure 6. The increase in displacement of the beams with the same number of CFRP layers due to prestressing force reduction

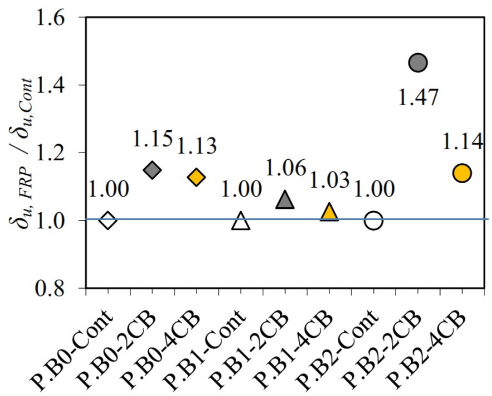

Figure 7. The increase in maximum displacement of the strengthened beams compared to control beams in the same group

CFRP sheets also increased deformation capacity (maximum displacement) of the strengthened beams compared to the un-strengthened beams, from 13% to 15% for Group 1, 3% to 6% for Group 2, and 14% to 47% for Group 3. The increase in deformation capacity also increased slightly in correlation with the number of CFRP layers (except the case of P.B2-2C) and with the prestressing force reduction (Fig. 7).

3.3. *The flexural strengthening effectiveness of CFRP sheets and energy absorption capacity*

CFRP sheets significantly improved the flexural capacity of the strengthened beams and which increased when the number of strengthening layers increased; however, the increase level in flexural capacity is inversely proportional with the number of strengthening layers and directly proportional with the prestressing force reduction levels (Fig. 8). In particular, at the serviceability state (which corresponds to the load levels when the beam displacement $\leq L/250 = 13.6$ mm), the flexural capacity increased on average 23% to 58% when the number of CFRP layers increased from 2 to 4 layers. At the ultimate state (corresponds to the load levels when the beam displacement $> L/250 = 13.6$ mm), the strengthening effectiveness of CFRP was more considerable,

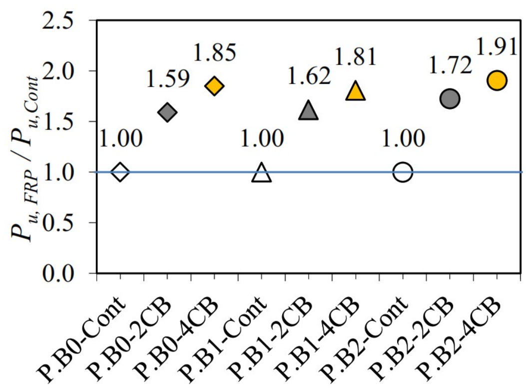

Figure 8. The increase in flexural capacity of the strengthened beams compared to the control beams in the same group

which was shown through an increase in flexural capacity from 59% to 85% for Group 1, 62% to 81% for Group 2, and 72% to 91% for Group 3 (Fig. 8). These results showed that the flexural strengthening effectiveness of CFRP sheets tends to increase with the decrease in prestressing force.

Furthermore, CFRP sheets also significantly improved the energy absorption capacity, E_b, of the beams (Table 4); accordingly, CFRP sheets increased E_b from 64% to 77% for Group 1, 52% to 59% for Group 2, and 98% to 147% for Group 3.

3.4. Cracking behavior

CFRP sheets showed their effectiveness in controlling cracks and delaying crack development; thereby drastically reducing the width of cracks in beams (Fig. 9). The more CFRP layers were used, the more reduction of crack widths was observed but with the reduction level became smaller. The flexural cracks of the strengthened beams appeared later than that of the reference beam. The cracking loads of the strengthened beams, $P_{cr,CFRP}$, in Group 1, 2, and 3 were greater than that of the reference beam 11%, 13%, and 11% respectively (Table 4). The number of CFRP layers had no obvious influence on the cracking loads; however, the reduction in prestressing force made the first flexural cracks appeared sooner. In particular, the cracking loads in Group 2 (15% prestressing force reduction) were smaller than that of the reference beam in Group 1: 11%, 10%, 10% for the un-strengthened beam, the beams strengthened with 2 and 4 CFRP layers respectively. Similarly, the cracking loads in Group 3 (30% prestressing force reduction) were approximately 20% smaller than that of Group 1.

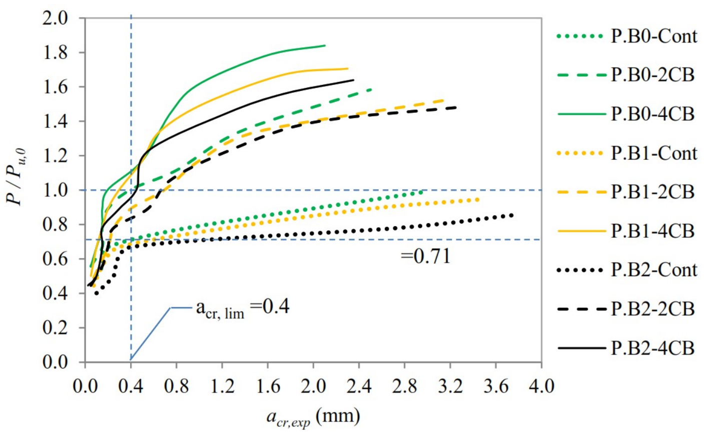

Figure 9. Relative load-crack width diagrams of the tested beams

At the load level that caused allowable cracks, $a_{cr,lim} = 0.4$ mm, of the un-strengthened beams ($0.71P_{u,0}$ for Group 1, $0.68P_{u,0}$ for Group 2 and $0.67P_{u,0}$ for Group 3 – Fig. 9), the widths of the largest crack measured on the strengthened beams were smaller than that of the un-strengthened beam: 63% to 71%, 70% to 74%, and 50% to 63% for Group 1, Group 2, and Group 3 respectively. At failure load of the control beams, $P_{u,Cont}$, the width of cracks in the strengthened beams were much smaller than in the control beams: 7.9 to 15.4 times, 6.4 to 14 times, and 8.3 to 14.9 times for Group 1, Group 2, and Group 3 respectively. Fig. 10(a) showed the width of cracks of the strengthened beams decreased gradually as the number of CFRP reinforcement layers increased. The reason is that the CFRP axial stiffness ($E_f A_f$) increased when the number of CFRP layers increased (E_f and A_f are the elastic modulus and cross-sectional area of CFRP sheets respectively), which reduced tensile stress of the CFRP sheets, thereby reduced the width of cracks in the beams. Similarly, at failure load of each beam, the maximum crack width of the strengthened beam was also significantly smaller than that of the un-strengthened beam: from 1.2 to 1.4 times, 1.1 to 1.5 times, and from 1.2 to 1.6 times for Group 1, Group 2, and Group 3 respectively (Fig. 10(b)). Most noticeably, the reduction level in width of cracks became smaller as the number of CFRP strengthening layers increased.

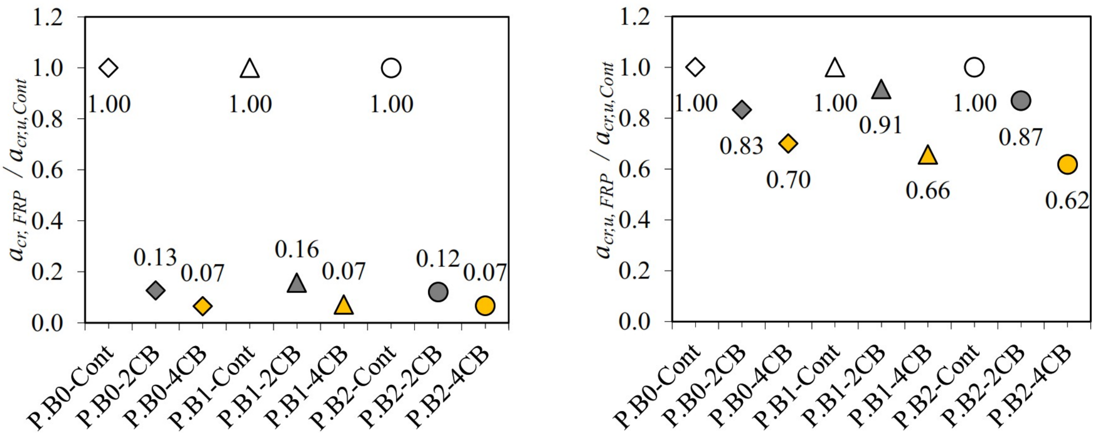

(a) At failure load of the control beams, $P_{u,Cont}$ (b) At failure load of each beam, $P_{u,exp}$

Figure 10. The reduction in crack widths of the CFRP-strengthened beams when compared to the control beam in the same group

For the beams with the same number of strengthening layers, in first phase before beams exceeded allowable displacement, beams with different prestressing force reduction level (0%, 15%, 30%) had almost the same load-crack width relationships. At the next load levels, when displacement exceeded allowable limits, the width of cracks increased as prestressing force reduction level increased. In particular, at the maximum loads of the beams with prestressing force reduction (Group 2 and 3), the width of cracks of these beams increased when compared to beams with no prestressing force reduction (Group 1): from 37% to 127%, 44% to 63%, and 74% to 118% for the un-strengthened beams, the beams strengthened with 2 and 4 CFRP layers respectively (Fig. 11).

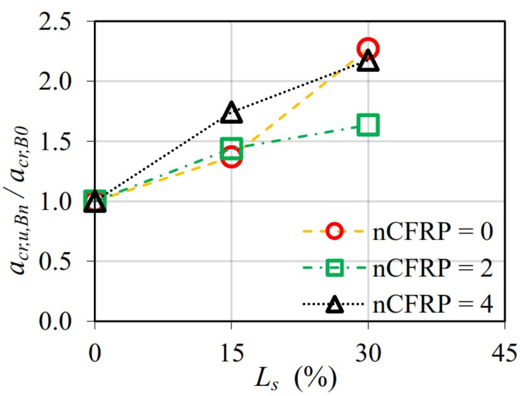

Figure 11. The increase in cracks widths of the beams with the same number of CFRP layers due to prestressing force reduction

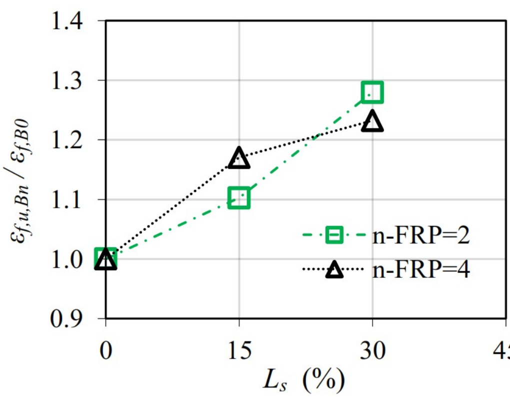

Figure 12. The increase in CFRP strain of the beams with the same number of CFRP layers due to prestressing force reduction

3.5. Strain in flexural-strengthening CFRP sheets and concrete

The relationships between the load and strain of the CFRP sheets are shown in Fig. 13. Before the cracking load (approximately 40% − 56% failure load of the control beam in Group 1, $P_{u,0}$), the strain of CFRP sheets was small, and it was not dependent on the number of CFRP layers and the prestressing force. After cracking load, CFRP sheets became more effective, the strain of the CFRP sheets increased significantly, but the increase was reduced when more CFRP layers were applied. The increase rates of strain in the CFRP sheets with and without prestressing force reduction were almost similar; however, at the same load level, the strain of CFRP sheets in beams with prestressing force reduction was greater than that of the reference beam. The maximum strain of CFRP sheets in beams strengthened with 2 and 4 CFRP layers were respectively 11.8‰ and 9.1‰ for Group 1, 12.6‰ and 9.8‰ for Group 2, and 13.2‰ and 9.2‰ for Group 3, which corresponded to 43% − 63% the rupture strain of the CFRP sheets (ε_{ffu} = 21‰). Thus, increasing CFRP strengthening layers from 2 to 4 layers significantly reduced the maximum strain of CFRP by an average of 25%. The maximum strain of the CFRP sheets reduced with the increase of the number of CFRP layers which resulted in a higher stiffness of the CFRP sheets as shown in the decrease in the slope of the load-strain of the CFRP sheets curves (Fig. 13).

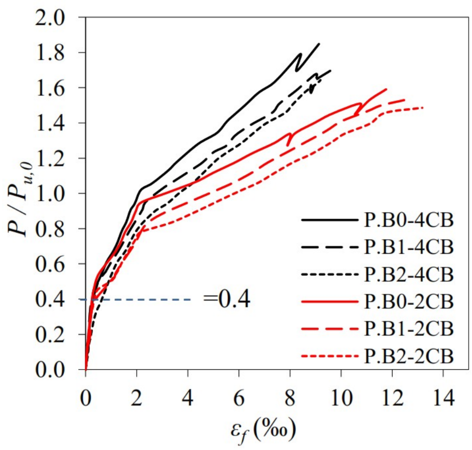

Figure 13. Relative load-strain diagrams of CFRP sheets at midspan

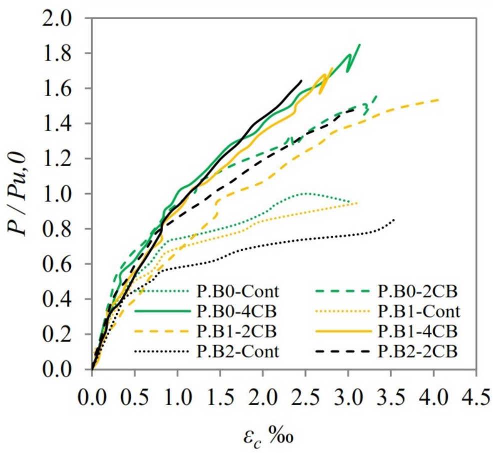

Figure 14. Relative load-compressive strain diagrams of concrete at midspan

When considering beams with the same number of strengthening layers, in the first phase before beams exceeded allowable displacement ($L/250$ = 13.6 mm), the strain of CFRP sheets in the beams with different prestressing force reduction levels (0%, 15%, 30%, corresponding to Group 1, 2, and 3) were almost the same. However, at the next load levels, when displacement exceeded allowable limits, the strain of CFRP at midspan of beam tended to increase as prestressing force reduction level increased. In particular, at the maximum loads of the beams with prestressing force reduction (Group 2 and 3), the strain of CFRP sheets in these beams increased when compared to beams with no prestressing force reduction (Group 1): from 10% to 28% and 17% to 23% for the beams strengthened with 2 and 4 CFRP layers respectively (Fig. 12). This phenomenon can be explained as the decrease of prestressing force led to a decrease in beam stiffness, and thus increased beam displacement, thereby led to an increase in strain of CFRP sheets.

The relationship between load and compressive strain of concrete are shown in Fig. 14. The relationship between load and concrete deformation was quite similar to the relationship between load and deflection. CFRP sheets significantly affected compressive strain of concrete. CFRP sheets, thanks to its cracking control mechanism, which helped restrict crack development (both width and length of cracks) in beams, as mentioned above (see section 3.4. Cracking behavior). This made the height of compressive zone in the cross section of the strengthened beams larger than that of the un-strengthened beams, which led to the less compressive concrete strain of the strengthened beams. In particular, at the maximum load of the un-strengthened beams, $P_{u,Cont}$, the compressive concrete strain in beams strengthened with 2 and 4 CFRP layers were smaller than that of the un-strengthened beams: from 53% to 60%, 53% to 66%, and 72% to 76% for Group 1, Group 2, and Group 3 respectively. The decreased level in concrete strain of the strengthened beams compared to the control beams became smaller as the number of CFRP strengthening layers increased. This could be explained as the cracking control effectiveness of CFRP sheets also diminished as the number of CFRP layers increased, as mentioned above.

3.6. Strain in tendons and longitudinal rebar, and interaction between CFRP sheets and tendons

Before the first crack appeared in beams, the tendons did not really work so the strain increases was negligible (<0.35‰). During this phase, tendon behavior in beams was almost similar. After cracks appeared (at the load levels about (40 – 56%)$P_{u,0}$) the tendons worked more effectively. The increase rates of tendon strain in the strengthened beams was smaller than that of the control beams at the same load level and tended to slow down as the number of CFRP strengthening layers increased (Fig. 15). At the load level which the width of cracks in the un-strengthening beams reached $a_{cr,lim}$ = 0.4 mm (71%$P_{u,0}$, 68%$P_{u,0}$ and 67%$P_{u,0}$ for Group 1, 2, and 3 respectively), the increase in tendon strain of the un-strengthening beam in Group 1 (P.B0-Cont) reached approximately 0.52‰; meanwhile, the increase in tendon strain of the beams strengthened with 2 and 4 CFRP layers in the same group was 0.35‰ and 0.34‰ respectively, corresponding to a reduction of 33% and 35% when compared to the un-strengthened beams. Similarly, for the strengthened beams in Group 2 and 3, accordingly, the strain in tendons of the beams strengthened with 2 and 4 CFRP layers decreased when compared to the control beam were respectively: 37% and 50% for Group 2; 32% and 56% for Group 3. At higher load levels, tendon strain of the strengthened beams tended to decrease more strongly. In particular, at failure load of the un-strengthened beams, $P_{u,Cont}$, the increase in tendon strain of the beams strengthened with 2 and 4 CFRP layers decreased when compared to the control beam were

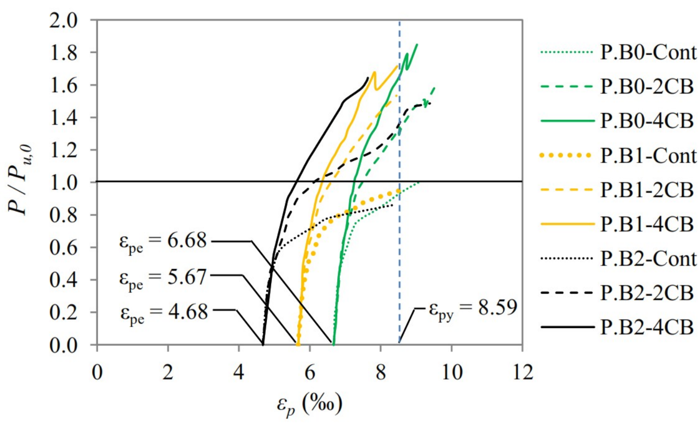

Figure 15. Relative load-strain diagrams of tendon at midspan

respectively: 66% and 76% for Group 1, 73% and 79% for Group 2, and 76% and 82% for Group 3. This reduction tended to be directly proportional to the reduction of prestressing force in the beams.

These results indicated that CFRP sheets had strong and positive effects on the behavior of the tendons during the beam working process. Thanks to the cracking control mechanism as previously mentioned, CFRP sheets slowed down the degradation of the beam stiffness, thereby helped the tensile stress in the beams was more uniformly distributed, minimized possible localized damage in concrete and the tendons. This helped to reduce the strain in tendons and, more importantly, helped to delay the point occurring nominal yield strain in tendons as shown in Fig. 16. According to Fig. 16, considering

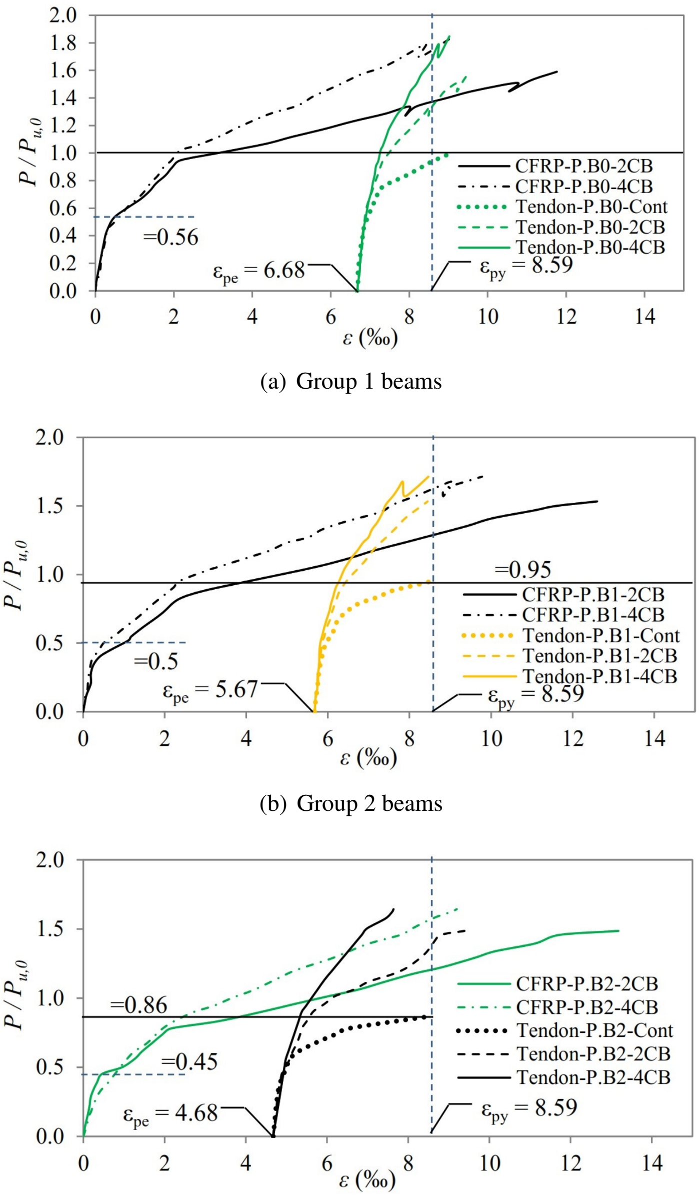

(a) Group 1 beams

(b) Group 2 beams

(c) Group 3 beams

Figure 16. Interaction between strain of CFRP and tendon of the tested beams

the Group 1, using 2 and 4 layers of CFRP strengthening increased the nominal yielding load by 40% and 77% respectively, when compared to control beam. The tested beams in Group 2 and 3, except for beam P.B2-2CB which had its tendons exceeded the yield strain at the ultimate loads (9.4‰), the maximum tendon strain in the rest of the beams were all smaller than the nominal yield strain around 1% to 11%. The maximum tendon strain decreased in direct proportion with the decrease in prestressing force. In particular, considering the un-strengthened beams, the decrease of 15% and 30% in prestressing force led to the reduction in maximum tendon strain by 6% and 8% respectively; likewise, for the beams strengthened with 2 CFRP layers, the decrease of 15% and 30% in prestressing force led to the reduction in maximum tendon strain by 11% and 2% respectively; and finally for the beams strengthened with 4 CFRP layers, the decrease of 15% and 30% in prestressing force led to the reduction in maximum tendon strain by 6% and 15% respectively (Fig. 17).

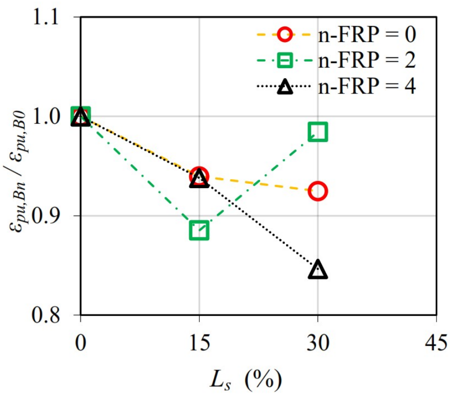

Figure 17. The decrease in maximum tendon strain of the beams with the same number of CFRP layers due to prestressing force reduction

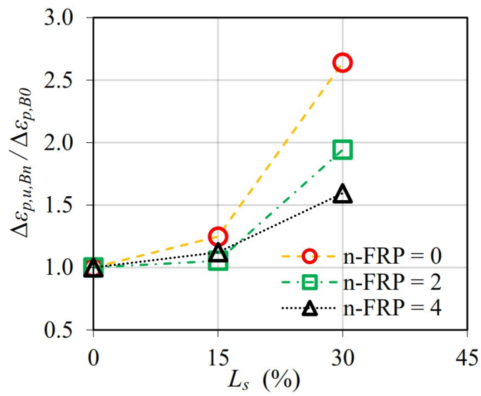

Figure 18. The increase in tendon strain of the beams with the same number of CFRP layers due to prestressing force reduction

In beams with the same number of strengthening layers, in the first phase before beams exceeded allowable displacement ($L/250 = 13.6$ mm), beams with different prestressing force reduction level (0%, 15%, 30% corresponding to Group 1, 2, and 3) had almost the same behavior. However, at the load levels bigger than P_{ser}, when displacement exceeded allowable limits, the increase in tendon strain tended to increase as prestressing force reduction level increased. In particular, at the maximum loads of the beams with prestressing force reduction (Group 2 and 3), the increase in tendon strain of these beams was greater when compared to the beams with no prestressing force reduction (Group 1): from 44% to 164%, 2% to 94% and 33% to 59% for the un-strengthened beams, the beams strengthened with 2 and 4 CFRP layers respectively (Fig. 18). It can be seen that as the number of strengthening layers increased, the effect of prestressing force reduction on the increase in tendon strain of the beams became smaller, which again proved the effectiveness of CFRP sheets as mentioned above.

Longitudinal rebars in the un-strengthened beams, the beams strengthened with 2 and 4 CFRP layers reached the nominal yield strain at load levels approximately $55 - 65$ kN, $70 - 85$ kN, and $85 - 105$ kN respectively. This result showed that strengthening 2 and 4 layers of CFRP helped increase nominal yielding load in longitudinal rebars by approximately $27 - 31\%$ and $55 - 62\%$ respectively when compared to the un-strengthening beams. In other words, CFRP sheets delayed the point occurring nominal yield strain of rebar and indirectly increased beam stiffness, which in turn led to better cracking control and decreased the beam displacement as mentioned above. For the beams strengthened with CFRP sheets, at the maximum load, the value of longitudinal rebar strain fluctuated between 15.1‰ and 33.5‰ (Table 4).

4. Conclusions

This paper conducted an experimental study on the effects of the changes in prestressing force due to prestressing force reduction on the flexural strengthening effectiveness of CFRP sheets for UPC beams. The testing program was carried out on nine large-scale UPC rectangular beams. The investigated parameters included the reduction of prestressing force (0%, 15%, and 30%) and the number of CFRP layers (0, 2, and 4 layers). Based on the results from this study, some conclusions can be drawn as follows:

- The flexural strengthening effectiveness of CFRP sheets for UPC beams was influenced greatly by the magnitude of prestressing force and the number of CFRP layers; accordingly, the strengthening effectiveness of CFRP sheets tended to increase as prestressing force reduction increased but decreased as the number of CFRP sheets decreased. The flexural capacity of UPC beams strengthened by 2 and 4 CFRP layers using anchored with CFRP U-wrapped uniformly distributed within the shear span greatly increased from 59% to 85% for the beams with no prestressing force reduction; 62% to 81% for the beams with 15% prestressing force reduction; and 72% to 91% for the beams with 30% prestressing force reduction;

- CFRP sheets significantly improved the energy absorption capacity of UPC beams (from 64% to 77% for the beams with no prestressing force reduction, from 52% to 59% for the beams with 15% prestressing force reduction, and from 98% to 147% for the beams with 30% prestressing force reduction), and this improvement was directly proportional with the decrease in the prestressing force in the beams. Besides, the prestressing force reduction also increased beam displacement (9% to 56%) but this increment diminished when the number of CFRP strengthening layers increased. CFRP sheets also greatly reduced the width of cracks in the beams by 50% to 74% at the serviceability state and 6.4 times to 15.4 times at the ultimate state;

- Tendons in UPC beams was greatly influenced by flexural-strengthening CFRP sheets; accordingly, CFRP sheets significantly reduced tendon strain (33% to 56% at the serviceability state and 66% to 82% at the ultimate state), and this reduction was directly proportional with the decrease in the prestressing force in the beams. The decrease in tendon strain helped to delay the point occurring nominal yield strain in tendons, in other words, CFRP sheets increased the capacity in nominal yield strength (40% to 77%). Besides, the prestressing force reduction also increased the additional strain of the tendons (44% to 164%), but decreased the maximum tendon strain (2% to 15%);

- The maximum strain of CFRP sheets in UPC beams tended to increase (from 10% to 28%) when prestressing force reduction increased but decreased when the number of CFRP strengthening layers increased. The maximum strain of CFRP in the tested beams fluctuated between 9.1‰ and 13.1‰, which corresponded to 43% to 63% the rupture strain of the CFRP sheets.

Acknowledgements

This research is funded by Vietnam National Foundation for Science and Technology Development (NAFOSTED) under grant number 107.01-2018.302.

References

[1] Abdullah, A. B. M., Rice, J. A., Bhatia, R., Brenkus, N. R., Hamilton, H. R. (2017). Unbonded Tendons as an Alternative for Bonded Tendons in Post-Tensioned Bridges: Constructability, Structural Performance, and Monitoring. In *Structures Congress 2017*, American Society of Civil Engineers.

[2] Mieszczak, M. (2018). Unbonded prestressing tendons and their role in the construction of slender elements of buildings. *IOP Conference Series: Materials Science and Engineering*, 324:012017.

[3] Bakis, C. E., Bank, L. C., Brown, V. L., Cosenza, E., Davalos, J. F., Lesko, J. J., Machida, A., Rizkalla, S. H., Triantafillou, T. C. (2002). Fiber-Reinforced Polymer Composites for Construction—State-of-the-Art Review. *Journal of Composites for Construction*, 6(2):73–87.

[4] Nanni, A. (1995). Concrete repair with externally bonded FRP reinforcement. *Concrete International*, 17 (6):22–26.

[5] Hassan, T., Rizkalla, S. (2002). Flexural Strengthening of Prestressed Bridge Slabs with FRP Systems. *PCI Journal*, 47(1):76–93.

[6] Nguyen-Minh, L., Phan-Vu, P., Tran-Thanh, D., Truong, Q. P. T., Pham, T. M., Ngo-Huu, C., Rovňák, M. (2018). Flexural-strengthening efficiency of cfrp sheets for unbonded post-tensioned concrete T-beams. *Engineering Structures*, 166:1–15.

[7] Huynh-Xuan, T., Do-Dai, T., Ngo-Thanh, T., Pham, T. M., Nguyen-Minh, L. (2021). Effect of Sulfate Attack on Reinforced Concrete Columns Confined with CFRP Sheets under Axial Compression. *Journal of Composites for Construction*, 25(6):04021049.

[8] Tan, N. N., Kien, N. T., Giang, N. H. (2021). Numerical study on the flexural performance of RC beams with externally bonded CFRP sheets. *Journal of Science and Technology in Civil Engineering (STCE) - HUCE*, 15(4):182–196.

[9] Reed, C. E., Peterman, R. J. (2004). Evaluation of Prestressed Concrete Girders Strengthened with Carbon Fiber Reinforced Polymer Sheets. *Journal of Bridge Engineering*, 9(2):185–192.

[10] Rosenboom, O., Hassan, T. K., Rizkalla, S. (2007). Flexural behavior of aged prestressed concrete girders strengthened with various FRP systems. *Construction and Building Materials*, 21(4):764–776.

[11] Rosenboom, O., Walter, C., Rizkalla, S. (2009). Strengthening of prestressed concrete girders with composites: Installation, design and inspection. *Construction and Building Materials*, 23(4):1495–1507.

[12] Kim, Y. J., Green, M. F., Fallis, G. J. (2008). Repair of Bridge Girder Damaged by Impact Loads with Prestressed CFRP Sheets. *Journal of Bridge Engineering*, 13(1):15–23.

[13] Ludovico, M. D., Prota, A., Manfredi, G., Cosenza, E. (2010). FRP Strengthening of Full-Scale PC Girders. *Journal of Composites for Construction*, 14(5):510–520.

[14] Cerullo, D., Sennah, K., Azimi, H., Lam, C., Fam, A., Tharmabala, B. (2013). Experimental Study on Full-Scale Pretensioned Bridge Girder Damaged by Vehicle Impact and Repaired with Fiber-Reinforced Polymer Technology. *Journal of Composites for Construction*, 17(5):662–672.

[15] Kasan, J. L., Harries, K. A., Miller, R., Brinkman, R. J. (2014). Repair of Prestressed-Concrete Girders Combining Internal Strand Splicing and Externally Bonded CFRP Techniques. *Journal of Bridge Engineering*, 19(2):200–209.

[16] Nguyen, T. T. D., Matsumoto, K., Sato, Y., Iwasaki, A., Tsutsumi, T., Niwa, J. (2014). Effects of Externally Bonded CFRP Sheets on Flexural Strengthening of Pretensioned Prestressed Concrete Beams Having Ruptured Strands. *Journal of JSCE*, 2(1):25–38.

[17] Afefy, H. M., Sennah, K., Cofini, A. (2016). Retrofitting Actual-Size Precracked Precast Prestressed Concrete Double-Tee Girders Using Externally Bonded CFRP Sheets. *Journal of Performance of Constructed Facilities*, 30(2):04015020.

[18] Pino, V., Nanni, A., Arboleda, D., Roberts-Wollmann, C., Cousins, T. (2017). Repair of Damaged Prestressed Concrete Girders with FRP and FRCM Composites. *Journal of Composites for Construction*, 21 (3):04016111.

[19] Larson, K. H., Peterman, R. J., Rasheed, H. A. (2005). Strength-Fatigue Behavior of Fiber Reinforced Polymer Strengthened Prestressed Concrete T-Beams. *Journal of Composites for Construction*, 9(4): 313–326.

[20] Rosenboom, O., Rizkalla, S. (2006). Behavior of Prestressed Concrete Strengthened with Various CFRP Systems Subjected to Fatigue Loading. *Journal of Composites for Construction*, 10(6):492–502.

[21] Miller, A., Rosenboom, O., Rizkalla, S. (2006). Fatigue Behavior of Impact Damaged Prestressed Concrete Bridge Girder Repaired With Cfrp Sheets. In *7th International Conference on Short and Medium Span Bridges*, 1–10.

[22] Rasheed, H. A., Larson, K. H., Peterman, R. J. (2006). Analysis and Design Procedure for FRP-Strengthened Prestressed Concrete T-Girders Considering Strength and Fatigue. *Journal of Composites for Construction*, 10(5):419–432.

[23] ElSafty, A., Graeff, M. K., Fallaha, S. (2014). Behavior of Laterally Damaged Prestressed Concrete Bridge Girders Repaired with CFRP Laminates Under Static and Fatigue Loading. *International Journal of Concrete Structures and Materials*, 8(1):43–59.

[24] Chakrabari, P. R. (2005). Behavior of Un-Bonded Post-Tensioned Beams Repaired and Retrofitted with Composite Materials. In *Structures Congress 2005*, American Society of Civil Engineers.

[25] Meski, F. E., Harajli, M. (2013). Flexural Behavior of Unbonded Posttensioned Concrete Members Strengthened Using External FRP Composites. *Journal of Composites for Construction*, 17(2):197–207.

[26] Meski, F. E., Harajli, M. (2015). Evaluation of the Flexural Response of CFRP-Strengthened Unbonded Posttensioned Members. *Journal of Composites for Construction*, 19(3):04014052.

[27] Ghasemi, S., Maghsoudi, A. A., Bengar, H. A., Ronagh, H. R. (2016). Sagging and Hogging Strengthening of Continuous Unbonded Posttensioned HSC Beams by NSM and EBR. *Journal of Composites for Construction*, 20(2):04015056.

[28] Tran, D. T., Phan-Vu, P., Pham, T. M., Dang, T. D., Nguyen-Minh, L. (2020). Repeated and Post-Repeated Flexural Behavior of Unbonded Post-Tensioned Concrete T-Beams Strengthened with CFRP Sheets. *Journal of Composites for Construction*, 24(2):04019064.

[29] Phan-Vu, P., Tran, D. T., Pham, T. M., Dang, T. D., Ngo-Huu, C., Nguyen-Minh, L. (2021). Distinguished bond behaviour of CFRP sheets in unbonded post-tensioned reinforced concrete beams versus single-lap shear tests. *Engineering Structures*, 234:111794.

[30] ACI 440.2R-17 (2017). *Guide for the design and construction of externally bonded FRP systems for strengthening concrete structures*. American Concrete Institute, Farmington Hills, MI.

[31] CNR DT200R1 (2013). *Guide for the Design and Construction of Externally Bonded FRP Systems for Strengthening Existing Structures - Materials, RC and PC structures, masonry structures*. National Research Council (CNR), Rome.

[32] TR 55 (2012). *Design guidance for strengthening concrete structures using fibre composite materials*. The Concrete Society, Camberley, UK.

[33] Abdelrahman, A. A., Nofel, N. M., Ghallab, A. H., El-Afandy, T. H., Mahmoud, A. (2011). Behavior of prestressed concrete beams subjected to fire. *Housing and Building National Research Centre Journal*, 7:38–55.

[34] Zhao, H., Zeng, M., Chen, H., Ling, J., Wu, D. (2020). Investigating the Effect of Prestress Force on Cross-Tensioned Concrete Pavement Vibration. *Transportation Research Record: Journal of the Transportation Research Board*, 2674(8):875–886.

[35] Abdel-Jaber, H., Glisic, B. (2019). Monitoring of prestressing forces in prestressed concrete structures—An overview. *Structural Control and Health Monitoring*, 26(8).

[36] Kim, M. S., Lee, Y. H. (2020). Flexural Behavior of Posttensioned Concrete Beams with Unbonded High-Strength Strands. *Advances in Materials Science and Engineering*, 2020:1–12.

[37] Tang, C., Zhang, G., Song, C., Li, X., Hou, Y. (2021). Flexural Behavior of Unbonded Prestressed Concrete Bridge Girders. *Advances in Civil Engineering*, 2021:1–12.

[38] Naaman, A. E. (2004). *Prestressed Concrete: Analysis and Design*. Techno Press, Michigan, USA.

[39] O'Flaherty, F., Elomari, I. R., Lambert, P. (2017). Corrosion induced losses in pre-stressed tendons. In *37th Cement and Concrete Science Conference, 11-12 September 2017*, University College London.

[40] ACI 318 (2019). *Building Code Requirements for Structural Concrete*. American Concrete Institute, Farmington Hills, MI.